*Energy Equip. Sys./ Vol. 12/No. 4/December 2024/* 379-398

ENERGY EQUIPSYS

**Energy Equipment and Systems**

www.energyequipsys.com

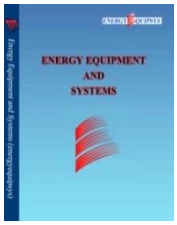


# Design and performance assessment of a novel ammonia-fueled integrated CHP-Based multigeneration system regarding to various EGR ratios: An energy approach

**Manuscript Type**
Research Paper

**Authors**

**Alireza Pirmohamadi**[a*]
**Behrooz M. Ziapour** [a]

[a]Department of Mechanical Engineering, University of Mohaghegh Ardabili, Ardabil, Iran.

*Article history*:

Received : 26 January 2024
Revised : 4 February 2024
Accepted : 8 February 2024

**ABSTRACT**

*Recently, there has been a growing focus on the implementation of integrated energy systems using low-carbon fuels to align with sustainability objectives. This study conducted an investigation into a novel CHP system, which was designed to meet the efficient energy production. This innovative system utilized the ammonia fuel within Brayton cycle, incorporating various interconnected subsystems, including the Kalina cycle, High-Temperature Steam Electrolysis, ultra supercritical steam Rankine cycle as well as ammonia synthesis reactor. The primary aim of this system was to reduce dependence on external resources by establishing local sources for water and fuel, thus enhancing energy sustainability. Using Gaseq and EES software, thermochemistry and thermodynamic models of the integrated system was developed, providing valuable insights into the interactions among system parameters. In-depth investigations involved the examination of different energy system scenarios. The results revealed the superiority of the integrated system with a remarkable thermal efficiency of 47.8% and a net power generation of 2.65 MW, in contrast to the ammonia Brayton cycle with power generation of 1.43 MW and an efficiency of 28.7%. This study also highlighted the environmental benefits of the ammonia Brayton system by zero carbon and under 10 ppm NOx emission, showcasing its significant environmental sustainability.*

**Keywords:** CHP, Ammonia, Brayton Cycle, EGR, Hydrogen Production, HTSE.

## 1. Introduction

In recent decades, there has been a remarkable surge in global energy demand, primarily driven by population growth, industrial development, and technological advancements [1]. Simultaneously, concerns about the environmental consequences of energy production and consumption are posing a significant challenge [2]. Addressing both the escalating energy demand and the imperative to mitigate environmental impacts has led to a paradigm shift in energy production and utilization.

In this context, Integrated systems have emerged as a promising solution. These systems, characterized by their integrated production of electricity, heat, cooling, and

* Corresponding author: Alireza Pirmohamadi
Department of Mechanical Engineering, University of Mohaghegh Ardabili, P.O. Box 179, Ardabil, Iran.
E-mail address: Pirmohamadi.ar@uma.ac.ir

other valuable products from a singular energy source, offer a potential avenue to enhance energy efficiency and alleviate negative environmental impacts [3] [4].

Integrated energy systems present a comprehensive approach to optimizing the use of primary energy sources, leading to substantial reductions in issues such as carbon dioxide emissions, air pollutants, and resource depletion [5]. Their inherent ability to generate various forms of energy and significant products positions them as a desirable option for achieving a sustainable energy supply. These systems encompass a diverse range of technologies and configurations, including combined heat and power (CHP) systems, trigeneration, polygeneration systems [6].

Power generation is the basis of an integrated system, providing the necessary operational support for its various subsystems. Within the realm of power generation systems, Brayton cycles in diverse configurations have conventionally played a crucial role. In recent years, the quest for alternative fuels in these energy systems has gained significant traction, driven by the growing demand for sustainable and environmentally friendly energy solutions [7].

Amidst the alternative fuels explored in the literature, ammonia fuel have emerged as a particularly promising option for enhancing Brayton systems. While methane's role as a hydrocarbon fuel in energy production is well-established, the replacement of methane with ammonia, renowned for its potential as an energy carrier and low emissions, offers a pathway to reducing emissions in Brayton cycles [8].

In the landscape of research on new fuels in gas turbines, much of the focus has been on the chemical properties of combustion and their impact on flue gas contents and efficiency. For instance, Avila et al. [9] conducted an experimental assessment of a commercial ammonia-methane gas turbine. Their findings indicated stable operation with an ammonia fraction of up to $X_{NH3}$=0.63, albeit with an increase in NOx and $N_2O$ particles. However, the use of ammonia-methane fuel, in comparison to pure methane, resulted in a slightly lower thermal efficiency of 23%.

Another study by Xiao et al. [10] proposed the ammonia-based fuel mixture under rich combustion conditions. They advocated for ammonia as a methane substitute in power generation. The introduction of enriched oxygen into the combustion chamber increased thermal efficiency without a concurrent rise in emissions. Additionally, the study investigated various reduced combustion mechanisms for ammonia-based flames and considered their implications for gas turbine design.

Valera-Medina et al. [11] examined the details of ammonia-based mixture combustion in a gas turbine system, employing tangential swirl-shaped burners. Their investigation explored various equivalence ratios under reference pressure, utilizing numerical simulations to unravel species progression in the ammonia mixture. The findings underscored the inefficiency of fully premixed injection for ammonia combustion, emphasizing the need for lower swirl and an alternative injection approach to enhance power generation with ammonia fuel.

In a novel approach, Keller et al. [12] proposed a combined energy system that harnessed the potential of flue gas recycling through an EGR unit to optimize ammonia as a fuel in power generation. This innovative arrangement not only increased power output but also elevated thermal efficiency by combusting the hydrogen in the flue gas within the HRSG. The study highlighted the critical factors influencing the system performance, including TIT, EGR ratio, and the permissible NOx value in the flue gas. Their results emphasized the necessity of low-temperature EGR for maintaining stability in both thermal efficiency and NOx levels.

Pirmohamadi and Ziapour [13] took an integrated approach by proposing ammonia and methane/hydrogen Brayton cycles with an EGR component. Their comprehensive energetic and environmental analyses yielded optimal fuel mixture fractions, a reduction in combustion temperature, and a notable improvement in overall thermal efficiency from 63% to 74%. Numerous other studies have also delved into the utilization of ammonia as a fuel or a component of fuel mixtures, as referenced in [14], [15], [16], [17], [18], [19], [20], [21], [22].

Moreover, as indicated by the existing literature, diverse integrated subsystems have been utilized for the production of process

byproducts, encompassing hydrogen, ammonia, water, and other essential utilities. This configuration transforms the entire system into a sustainable design with an efficient setup. In this context, we provide a brief overview of relevant literature:

Yilmaz et al. [23] proposed a polygeneration plant that produces power, hydrogen, ammonia, and fresh water. The integrated plant comprised subsystems of Brayton and Rankine cycles, HTSE, and ASR processes. Thermodynamic and environmental analyses calculated energy and exergy efficiencies at 52% and 70%, respectively, with an overall $CO_2$ emission rate of 11.4 kg/kWh. In another study [24], they conducted similar analyses on a polygeneration system integrating a gas turbine and water desalination, finding optimal energy and exergy efficiencies of 60% and 56%, respectively.

He et al. [25] explored a solar HTSE process for hydrogen production within a multigeneration configuration. The integrated subsystems involved a parabolic solar system, a storage tank, and an HTSE process. The thermodynamic evaluation revealed total energetic and exergetic efficiencies of 21.5% and 22.5%, respectively. AlZahrani and Dincer [26] proposed an HTSE process with a well-performing conversion rate and profitable pure hydrogen supply, conducting an inclusive exergoeconomic analysis.

Anvari et al. [27] investigated an improved integrated system for power, heating, cooling, and distilled water production using various thermodynamic and environmental approaches. The integrated subsystems included a heat and power cogeneration system, an absorption chiller, and a water desalination process. The environmental assessment showed a $CO_2$ emission index of 0.16 kg/kWh, with calculated power and heat generation rates of 30.5MW and 41MW, respectively.

Eldeib et al. [28] proposed an energy system integrating solar and biomass energies to meet the needs of a dairy farm. Subsystems aimed at power, treated water, heating, cooling, and more. Thermodynamic analysis revealed energy and exergy efficiencies of about 81% and 43%, respectively. Numerous related studies are referenced, including [29], [30], [31], [32], [33], [34], [35], [36].

Despite the wealth of literature, no CHP integrated system with ammonia fuel has been identified where the process design achieves on-site production of all operational requirements such as ammonia and nitrogen, etc. Additionally, in the industrial scale, the use of ammonia fuel is rarely explored in the literature. In this study, we present a novel CHP system drived by an ammonia Brayton cycle where waste heat operates subsystems through heat exchangers and HRSG. These subsystems provide additional electricity and produce required hydrogen, nitrogen and ammonia. They include the Kalina cycle, USC steam Rankine cycle, HTSE, as well as ASR processes. The primary objective is to enhance power generation and increase the efficiency of the proposed system. The subordinate aims of this research are multifold, and include:

- Presenting a novel ammonia fueld Brayton cycle as the driving system
- Modeling integrated subsystems and calculating thermochemistry and thermodynamic properties
- Developing codes for energy analysis, conducting a parametric study, and finding the optimal features of the proposed integrated system.
- Conducting the energy analysis to overall plant.
- Investigateing the impacts of EGR and equivalence ratio on performance of the subsystems and the overall plant.

Subsequent sections will investigated the system description, system model design, methodology, results, and discussion, aiming to uncover new insights into the progression of novel energy systems within the context of sustainable production.

## Nomenclature

| | |
|---|---|
| h | Specific enthalpy (kJ/kg) |
| $\dot{m}$ | mass flow rate (kg/s) |
| P | Pressure (bar) |
| $\dot{Q}$ | Heat load rate (kW) |
| s | Specific entropy (kJ/kg.K) |
| T | Temperature (K) |
| $\dot{W}$ | Work/power rate (kW) |
| x | molar fraction |
| $X_b$ | Basic Ammonia concentration (%) |

## Subscripts and Superscripts

| | |
|---|---|
| AC | Air Compressor |

| | |
|---|---|
| BC | Brayton Cycle |
| CC | Combustion Chamber |
| c | Cold flow |
| f | fuel |
| GT | Gas Turbine |
| h | Hot flow |
| H | Hot temperature |
| in | Inlet condition |
| i | Component |
| KC | Kalina Cycle |
| L | Cold temperature |
| out | outlet condition |
| pum | pump |
| P | product |
| regen | Regenerator |
| R | reactant |
| sep | Separator |
| sys | System |
| s, is | isentropic |
| tot | total |
| 0 | Reference environment condition |

### Abbreviations

| | |
|---|---|
| ASR | Ammonia Synthesis Reactor |
| ATF | Air-to-fuel ratio |
| CV | Control volume |
| HC | Hydrogen Compressor |
| HEX | Heat Exchanger |
| HTSE | High-Temperature Steam Electrolysis |
| LHV | Lower Heating Value |
| NC | Nitrogen Compressor |
| PR | Pressure Ratio |
| TIT | Turbine inlet temperature |
| TUR | Turbine |
| TER | Turbine expansion ratio |
| tv | Throttle valve |
| USC | Ultra Supercritical |
| ST | Steam Turbine |

### Greek letters

| | |
|---|---|
| $\Delta$ | Difference |
| $\varepsilon$ | Regenerator effectiveness |
| $\varphi$ | Equivalence ratio |
| $\eta_{th}$ | Thermal efficiency (%) |

## 2. System description

This research introduces an innovative self-sufficient energy system that, while initially dependent on external sources for working fluids like water and fuels, becomes self-sustaining over time with on-site provision of these essentials. The system utilizes ammonia fuel consisting of ammonia within a Brayton cycle, powering various interconnected subsystems. The integration of Brayton, USC steam Rankine and Kalina cycles generates the required power.

Moreover, the High-Temperature Steam Electrolysis (HTSE) system facilitates hydrogen production. The produced hydrogen, is utilized in ammonia synthesis reactor (ASR) to produce ammonia, contributing to the fuel of the Brayton cycle. Additionally, an Ammonia Synthesis Reactor (ASR) employs nitrogen which is produced from flue gas components of the Brayton cycle.

In essence, the ammonia Brayton cycle propels all the mentioned interconnected subsystems. The schematic of this proposed integrated system is depicted in Fig. 1. To deeper investigation of each subsystem, the following sections provide a comprehensive explanation.

### 2.1. Ammonia Brayton cycle

In our pursuit of environmentally friendly power systems characterized by appropriate thermal efficiency and straightforward configurations, we have chosen the ammonia Brayton cycle as the driving cycle for the proposed integrated plant, as illustrated in Fig. 1, based on the work by Keller et al. [12]. This cycle serves as the driving force in our overall system and encompasses key components typical of a basic Brayton system, including a compressor, a combustion chamber, and an expanding turbine.

Initially, a specific volume of air is drawn into the air compressor under reference conditions. However, subsequent loops involve modifications to this air, with the Exhaust Gas Recirculation (EGR) unit circulating predominantly nitrogen-containing exhaust gases from the cycle. In the second stage, a combustion chamber becomes the focal point where the ammonia-air mixture undergoes combustion. Achieving complete combustion of the ammonia fuel mixture results in an extremely high temperature, around 2004 K, necessitating the use of heat-resistant materials. The third component is the turbine, where the high-temperature combustion products expand, converting heat into mechanical work.

Recognizing the energy potential of exhaust gases in conventional gas turbine systems, we redirect the exhaust gases towards a Heat Recovery Steam Generator (HRSG) in the next

stage. Here, a portion of the remaining thermal energy is harnessed as the heat source for the bottoming USC steam Rankine cycle. Additionally, the residual waste energy will be harnessed through a dedicated heat exchanger (HEX2) to drive the Kalina cycle efficiently. Furthermore, a dryer unit will be employed to extract and drain water content as process water into the HSTE process. The remaining nitrogen gas, post-extraction, will be directed to the compressor through the Exhaust Gas Recirculation (EGR) unit. Simultaneously, a proportion of nitrogen will be stored in a dedicated $N_2$ storage tank to later supply the Nitrogen compressor(NC) for the ASR process.

Thermodynamic data for the ammonia cycle is sourced from the comprehensive study conducted by Keller et al. [12].

### 2.2. Ultra supercritical (USC) Steam Rankine cycle

As previously discussed, the steam Rankine cycle is powered by the Heat Recovery Steam Generator (HRSG) unit and incorporates the components of a basic Ultra-Supercritical (USC) Rankine cycle, as illustrated in Fig.1. This configuration enhances the overall power output in comparison to traditional combined cycle power plants when employed as a bottoming cycle for the ammonia cycle. The steam Rankine cycle consists of a backpressure steam turbine, a condenser, and a pump. Thermodynamic data for this cycle is sourced from the comprehensive research conducted by Keller et al. [12].

### 2.3. Ammonia-water Kalina cycle

The surplus waste energy produced by HEX2, a byproduct of the ammonia Brayton cycle, is effectively harnessed to drive the Kalina system (KC), thereby augmenting overall power generation through the KCT turbine. The foundation of this cycle is inspired by the work of Ghaebi et al. [37], utilizing an ammonia and water solution as the operational fluid. Its dual purpose lies in enhancing the primary ammonia Brayton cycle and elevating the overall system efficiency.

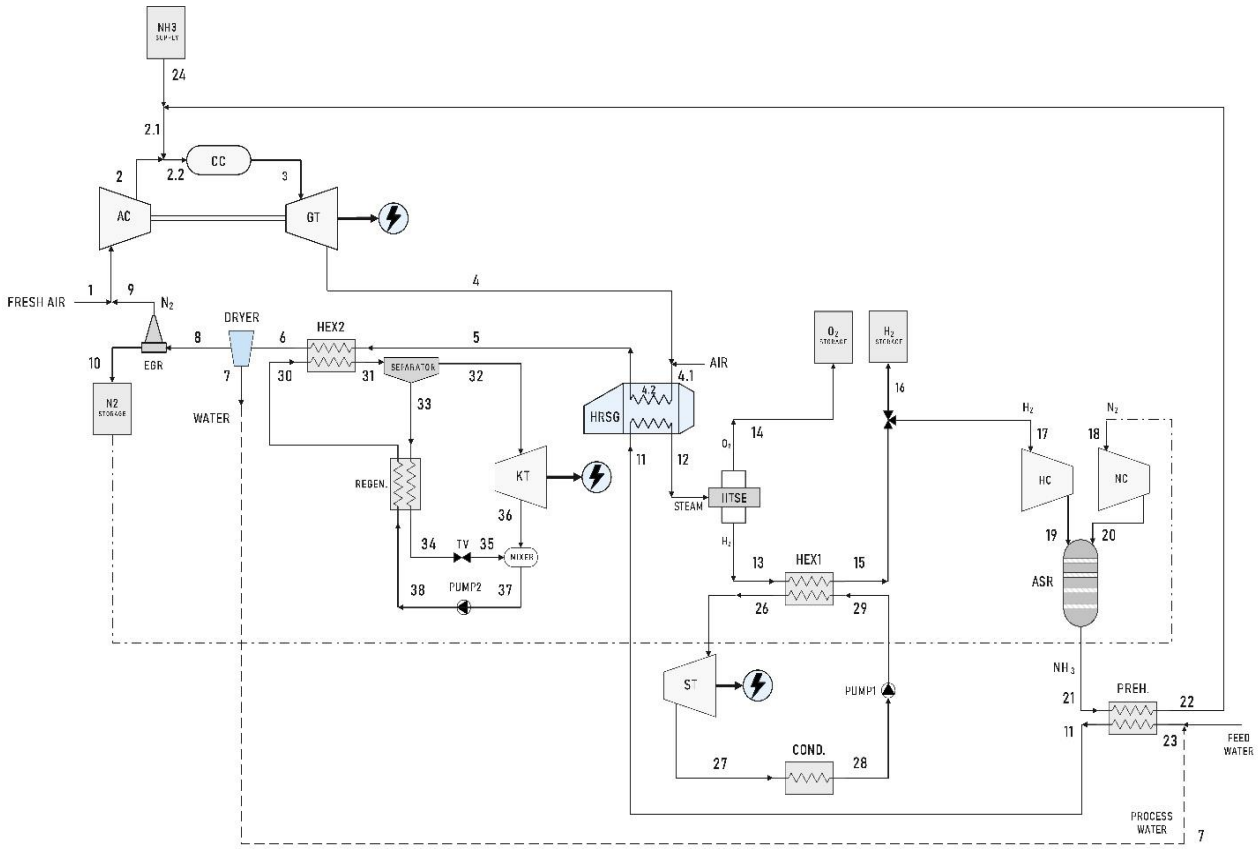


**Fig. 1.** Schematic of the proposed integrated system.

The key components of the Kalina cycle, illustrated in Fig.1, include a mixer, a regenerator, a throttling valve, a separator, a heat exchanger (HEX2), an expanding turbine, and a pump. The operation commences with the two-phase working solution, characterized by low pressure, entering HEX2, from where it proceeds to the separator. The vapor phase of the working fluid is separated and directed for expansion through the KCT turbine, generating power. Simultaneously, the depleted liquid mixture from the separator undergoes heat exchange in the regenerator, resulting in a temperature reduction. It then flows through the throttle valve, causing a pressure drop as it enters the mixer. At this juncture, the stream blends with the depleting fluid from the KCT turbine.

The saturated blend undergoes compression through a pump and subsequently enters the regenerator for heat exchange, completing the Kalina cycle loop via HEX2. This systematic process maximizes energy utilization and enhances the overall efficiency of the integrated system.

### 2.4. High-temperature steam electrolysis (HTSE)

The High-Temperature Steam Electrolysis (HTSE) system represents an exemplary Solid Oxide Electrolysis Cell (SOEC), for water steam electrolysis system, meticulously designed for hydrogen production within process plants. This innovative system is driven by the heat load of HRSG and the power demand of the plant. Its primary function is to efficiently separate water in its gaseous phase into hydrogen and oxygen at elevated temperatures, utilizing principles outlined in the work presented by Yilmaz et al. [23].

The process commences within the heat exchanger (HEX1), where high-temperature flue gas provides the necessary heat for water flowing from the preheater. This results in water steam at 900K entering the HTSE, as illustrated in Fig.1. While the heat required for the HTSE process is supplied by the Heat Recovery Steam Generator (HRSG) unit, the integrated system simultaneously meets the power demand of the electrolysis process.

During the electrolysis process, inlet steam is utilized, breaking down into oxygen and hydrogen at the outlets of the HTSE. A portion of the generated hydrogen is directed to hydrogen storage, while the remaining hydrogen proceeds to the hydrogen compressor (HC) for the ammonia synthesis process. Additionally, the oxygen produced during electrolysis is transferred to oxygen storage. This integrated approach ensures a seamless and efficient utilization of resources, making the HTSE system a key player in sustainable hydrogen production within industrial processes.

### 2.5. Ammonia Synthesis Reactor (ASR)

Ammonia production, as depicted in Fig.1, plays a pivotal role in realizing the envisioned multigeneration system. In this context, the hydrogen generated takes center stage as it is directed to the Hydrogen Compressor (HC) to contribute in the ammonia synthesis reaction. The foundational principles of the Ammonia Synthesis Reactor (ASR) subsystem are derived from the extensive research conducted by Yilmaz et al. [23].

The ASR process hinges on the utilization of hydrogen and nitrogen as the primary reactants for ammonia synthesis. The necessary hydrogen is produced within the High-Temperature Steam Electrolysis (HTSE) subsystem, while nitrogen is extracted from the Exhaust Gas Recirculation (EGR) unit and directed to the Nitrogen Compressor (NC). Achieving the requisite pressure of 150 bar for ammonia synthesis is accomplished through the coordinated operation of the Hydrogen and Nitrogen Compressors.

Following this, the generated ammonia undergoes condensation through a preheater, while the water supplied into the preheater for initial heating and is subsequently transferred to the Heat Recovery Steam Generator (HRSG) unit. Additionally, a portion of the produced ammonia is reserved for storage, serving various purposes such as acting as a liquid ammonia fertilizer in agriculture applications.

## 3. System model design

### 3.1. Assumptions and Restrictions

The feasibility of the proposed integrated CHP system is examined with the developed thermochemical and thermodynamic models

via GasEq simulation and EES codes. This procedure is conducted under certain assumptions and constraints:

- The integrated system operates in steady-state conditions.
- The proposed system and subsystems maintain the adiabatic processes in their control volumes.
- Pressure drops are presumed to be null within the heat exchangers and mixer.
- The working fluid in throttle valve is assumed to be isenthalpic.
- Pump, turbines and compressors operate with certain isentropic efficiencies.
- Heat losses through heat exchangers and piping are excluded.
- The contributions of kinetic and potential energies are disregarded.
- As a theoretical study, catalyst, reaction kinetics, and the transport process are not considered for ASR process.

In addition to the mentioned assumptions, several essential design parameters of the power cycles and the other processes are required for calculation of other thermodynamic parameters, which are listed in Tables 1–3.

**Table 1.** Essential design criteria of ammonia Brayton cycle **[12]**.

| Parameters | Value |
|---|---|
| Inlet air temperature, $T_1$ (K) | 294.15 |
| Inlet air pressure, $P_1$ (bar) | 1.1013 |
| Turbine Inlet temperature, TIT (K) | 2011 |
| Air compressor efficiency, $\eta_{com}$ (%) | 85 |
| Gas turbine efficiency, $\eta_{gt}$ (%) | 80 |
| Combustion chamber efficiency, $\eta_{cc}$ (%) | 98 |
| Pressure Ratio, PR | 20 |
| HRSG outlet temperature, $T_5$ (K) | 400 |

**Table 2.** Essential design criteria of Kalina cycle **[37]**.

| Parameters | Value |
|---|---|
| Reference temperature, $T_0$ (K) | 298.15 |
| Reference pressure, $P_0$ (bar) | 1.1013 |
| Inlet temperature of cycle, $T_{in,sep}$ (K) | 337.16 |
| Inlet pressure of cycle, $P_{in,sep}$ (bar) | 17.82 |
| Basic ammonia mass fraction, $X_b$ (%) | 90 |
| Regenerator effectiveness, $\varepsilon_{Reg}$ (%) | 95 |
| Turbine inlet pressure, $P_{in,tur2}$ (bar) | 35.7 |
| Turbine isentropic efficiency, $\eta_{is,tur2}$ (%) | 85 |
| Kalina pump isentropic efficiency, $\eta_{is,pum}$ (%) | 75 |
| Turbine expansion ratio, TER | 2 |

**Table 3.** Essential design criteria of ASR and HTSE processes **[23]**.

| Parameters | Value |
|---|---|
| HTSE inlet temperature, $T_{17}$ (K) | 900 |
| HTSE inlet pressure, $P_{17}$ (bar) | 1.1013 |
| ASR pressure, $P_{26}$ &$P_{28}$ (bar) | 150 |
| $N_2/H_2$ mass ratio in ASR | 4.58 |
| $N_2$ compressor efficiency, $\eta_{NC}$ (%) | 85 |
| $H_2$ compressor efficiency, $\eta_{HC}$ (%) | 85 |

### 3.2. Methodology

Within the framework of the outlined assumptions and constraints, a methodology is employed to determine the requisite thermodynamic properties for each state within the proposed integrated system. Fundamental to this process is an in-depth understanding of the thermochemistry governing the driving cycle, which serves as the foundation for the various subsystems. Thus, the initial step entails conducting a thermochemical analysis of the combustion of ammonia.

Subsequently, energy calculations for the Brayton and Kalina, USC Rankine cycles, the HTSE, and the ASR are executed in sequence. These comprehensive calculations carried out meticulously, serve to reveal essential insights into the mass and energy equations of the overall system. The resulting data and analyses, presented here, will be elaborated upon in a subsequent section to provide a detailed explanation of the performance of the system.

#### 3.2.1. Thermochemistry of combustion

Ammonia, characterized as a carbon-free fuel, has found practical application in micro gas turbines and industrial furnaces in recent years. However, its utility has been limited by its high ignition temperature and the production of nitrogen oxides (NOx), presenting substantial challenges. Amongst the numerous approaches for these issues, utilizing ammonia fuel has appeared as a remarkable solution. In this respect, accurately realizing of each fuel content is necessary. Consequently, through a simplified experimental reaction, we can explain the comprehensive combustion of a nitrogen-added ammonia-air mixture and outline the coefficients of the various species involved.

The chemical reaction in the various states of the ammonia Brayton cycle under complete combustion conditions is presented in Table 4.

Also, the equivalence ratio of mixture demonstrates a stoichiometric condition, $\varphi = 1.2$, and defines as [38]:

$$\varphi = \frac{F/A}{(F/A)_{stoic}} \tag{1}$$

where F and A denote the Fuel-Air ratio in the Brayton cycle. $\frac{F}{A}$ indicates the actual ratio, while $(F/A)_{stoic}$ represents the fuel-air ratio in the theoretical state when combustion is complete. Besides, calculation of air to fuel ratio $(ATF)$ is required for estimating the fuel and air and mass flow rates. In this regard, as the $ATF$ value for separate methane and ammonia combustion is not identical, a calculation for ammonia mixture is conducted, $ATF = 6.05$, and is expressed as follows [13]:

$$ATF_{stoic} = \frac{\varphi\, \dot{m}_{air}}{\dot{m}_{fuel}} \tag{2}$$

Also, the specific enthalpy and entropy of the states with various species can be calculated as follows:

$$h = \sum_i x_i h_i \tag{3}$$

$$s = \sum_i x_i s_i \tag{4}$$

where $x_i$ implies the molar fraction of $i$-th species.

**Table 4.** Chemical reactions of states in Ammonia Brayton cycle in φ=1.2 and EGR=0.295

| Chemical reactions | State |
|---|---|
| $2.5(O_2+3.76N_2)+4.89N_2$ | 1 |
| $2.5(O_2+3.76N_2)+4.89N_2$ | 2 |
| $4NH_3+2.5O_2+14.29N_2$ | 3 |
| $5H_2O+H_2+16.29N_2$ | 4 |
| $6H_2O+ 18.17N_2$ | 5 |
| $6H_2O+ 18.17N_2$ | 6 |
| $6H_2O$ | 7 |
| $18.17N_2$ | 8 |
| $0.295(18.17N_2)$ | 9 |
| $1-(0.295(18.17N_2))$ | 10 |

3.2.2. Thermodynamic of processes

3.2.2.1. Energy analysis

Thermodynamic properties characterizing various states of equipment or processes can be thoroughly defined by employing the governing equations. Among these equations, mass and energy balances proves a particular significance in estimating the system performance. Therefore, energy analysis of a thermodynamic cycle can be presented under steady state, steady flow circumstances as follows [39]:

$$\sum \dot{m}_{out} - \sum \dot{m}_{in} = 0 \tag{5}$$

$$\sum (\dot{m}X)_{out} - \sum (\dot{m}X)_{in} = 0 \tag{6}$$

$$\dot{Q}_{CV,out} - \dot{Q}_{CV,in} + \dot{W}_{CV,out} - \dot{W}_{CV,in} - \sum (\dot{m}h)_{out} + \sum (\dot{m}h)_{in} = 0 \tag{7}$$

A combination of Tables 1–3 and the mentioned equations yield the required energy and mass balance equations for each equipment, shown in Table 5. Furthermore, the further properties of the subsystems would be measured through the following equations:

$$\dot{W}_{net,BC} = \dot{W}_{GT} - \dot{W}_{AC} \tag{8}$$

$$\dot{W}_{GT} = \dot{m}_{GT}.W_{GT} \tag{9}$$

$$\dot{W}_{AC} = \dot{m}_{air}.W_{AC} \tag{10}$$

$$\dot{W}_{ST} = \dot{m}_{st}.(h_{26} - h_{27}) \tag{11}$$

where $W_{GT}$ and $W_{AC}$ can be calculated using the equations expressed in Table 5. Also, the input heat load of the proposed system with a certain fuel mass flow rate is expressed as follows:

$$\dot{Q}_{CC} = \dot{m}_{fuel} \times LHV \times \eta_{cc} \tag{12}$$

where $\dot{m}_{fuel}$ refers to mass flow rate of fuel, $\eta_{cc}$ is thermal efficiency of combustion chamber and equals to 0.98. Also, LHV, denoting the lower heating value of fuel is presumed to be 18.6 MJ/kg for ammonia [40].

Also, the HTSE is another subsystem in which the electrolyze process leads to decomposition of steam content. In order to production of hydrogen in HTSE, both the heat load and power are required. HTSE reaction is formulated as follows [12]:

$$(H_2O)_{steam} + \dot{Q}_{HTSE} + \dot{W}_{HTSE} \rightarrow H_2 + O_2 \tag{13}$$

Moreover, the ammonia synthesis reaction (ASR), is an exothermic reaction in which hydrogen, produced by HTSE, and is transferred through TEG modules. Subsequently, it is compressed to react with high pressure nitrogen, produced by $CO_2$ capture membrane, to produce synthetic ammonia. The ammonia synthesis reaction is represented as follows [23]:

$$N_2 + 3H_2 \rightarrow 2NH_3 + \dot{Q}_{ASR} \tag{14}$$

According to the above-mentioned equations and the information presented in Table 5 one can calculate the total net power of the proposed multigeneration system as bellow:

$$\dot{W}_{net,sys} = \dot{W}_{GT} + \dot{W}_{KCT} + \dot{W}_{ST} - \dot{W}_{AC} - \dot{W}_{HC} - \dot{W}_{NC} - \dot{W}_{HTSE} - \dot{W}_{PUM1} - \dot{W}_{PUM2} \tag{15}$$

3.2.2.2. Efficiencies of system and subsystems

The calculation of thermal efficiency for various subsystems requires the determination of the general ratio between useful output and energy input. The thermal efficiencies for the proposed subsystems can be formulated as follows:

$$\eta_{BC} = \frac{\dot{W}_{net,BC}}{\dot{Q}_{in}} \tag{16}$$

$$\eta_{KCT} = \frac{\dot{W}_{KCT}}{\dot{Q}_{HEX2}} \tag{17}$$

$$\eta_{ST} = \frac{\dot{W}_{ST}}{\dot{Q}_{HEX1}} \tag{18}$$

$$\eta_{SYS} = \frac{\dot{W}_{net,sys}}{\dot{Q}_{in} + \dot{Q}_{HRSG}} \tag{19}$$

**Table 5.** Mass and energy balance equations of equipment in the proposed system.

| Component | Mass balance | Energy balance | Auxiliary Eq.(1) | Auxiliary Eq.(2) |
|---|---|---|---|---|
| Air compressor, AC | $\dot{m}_1 = \dot{m}_2$ | $\dot{m}_1 h_1 + \dot{W}_{AC} = \dot{m}_2 h_2$ | $W_{AC} = \frac{h_1 - h_{2S}}{\eta_{is,AC}}$ | $h_2 = h_1 . \frac{h_1 - h_{2S}}{\eta_{is,AC}}$ |
| Combustion chamber, CC | $\dot{m}_2 + \dot{m}_{fuel} = \dot{m}_3$ | $\dot{m}_2 h_2 + \dot{Q}_{CC} = \dot{m}_3 h_3$ | $\dot{Q}_{CC} = \dot{Q}_{in}$ | |
| Gas turbine, GT | $\dot{m}_3 = \dot{m}_4$ | $\dot{m}_3 h_3 = \dot{m}_4 h_4 + \dot{W}_{GT}$ | $W_{GT} = \eta_{GT} . (h_3 - h_4)$ | $h_4 = h_3 . (h_3 - h_{4S}) . \eta_{is,GT}$ |
| HRSG | $\dot{m}_4 = \dot{m}_5$ $\dot{m}_{11} = \dot{m}_{12}$ | $\dot{m}_4 h_4 + \dot{m}_{11} h_{11} = \dot{m}_5 h_5 + \dot{m}_{12} h_{12}$ | $\dot{Q}_{HRSG} = \dot{m}_4 . (h_4 - h_5)$ | |
| HTSE | $\dot{m}_{12} = \dot{m}_{13} + \dot{m}_{14}$ | $\dot{m}_{12} h_{12} + \dot{Q}_{HTSE} + \dot{W}_{HTSE} = \dot{m}_{13} h_{13} + \dot{m}_{14} h_{14}$ | $\dot{Q}_{HTSE} = \dot{Q}_{HRSG}$ | |
| Hydrogen storage | $\dot{m}_{15} = \dot{m}_{16} + \dot{m}_{17}$ | $\dot{m}_{15} h_{15} = \dot{m}_{16} h_{16} + \dot{m}_{17} h_{17}$ | | |
| Hydrogen compressor, HC | $\dot{m}_{17} = \dot{m}_{19}$ | $\dot{m}_{17} h_{17} + \dot{W}_{HC} = \dot{m}_{19} h_{19}$ | $W_{HC} = \frac{h_{17} - h_{19S}}{\eta_{is,HC}}$ | $h_{19} = h_{17} . \frac{h_{17} - h_{19S}}{\eta_{is,HC}}$ |
| Nitrogen compressor, NC | $\dot{m}_{18} = \dot{m}_{20}$ | $\dot{m}_{18} h_{18} + \dot{W}_{NC} = \dot{m}_{20} h_{20}$ | $W_{NC} = \frac{h_{18} - h_{20S}}{\eta_{is,NC}}$ | $h_{20} = h_{18} . \frac{h_{18} - h_{20S}}{\eta_{is,NC}}$ |
| ASR | $\dot{m}_{19} + \dot{m}_{20} = \dot{m}_{21}$ | $\dot{m}_{19} h_{19} + \dot{m}_{20} h_{20} = \dot{m}_{21} h_{21} + \dot{Q}_{ASR}$ | | |
| Preheater | $\dot{m}_{21} = \dot{m}_{22}$ $\dot{m}_{23} = \dot{m}_{11}$ | $\dot{m}_{21} h_{21} + \dot{m}_{23} h_{23} = \dot{m}_{22} h_{22} + \dot{m}_{11} h_{11}$ | | |
| Ammonia storage | $\dot{m}_{22} = \dot{m}_{2.1} + \dot{m}_{24}$ | $\dot{m}_{22} h_{22} = \dot{m}_{2.1} h_{2.1} + \dot{m}_{24} h_{24}$ | | |
| HEX 2 | $\dot{m}_5 = \dot{m}_6$ $\dot{m}_{30} = \dot{m}_{31}$ | $\dot{m}_5 h_5 + \dot{m}_{30} h_{30} = \dot{m}_6 h_6 + \dot{m}_{31} h_{31}$ | $\dot{Q}_{HEX2} = \dot{m}_5 . (h_5 - h_6)$ | |
| Separator | $\dot{m}_{31} = \dot{m}_{32} + \dot{m}_{33}$ | $\dot{m}_{31} h_{31} = \dot{m}_{32} h_{32} + \dot{m}_{33} h_{33}$ | | |
| Kalina cycle turbine, KT | $\dot{m}_{32} = \dot{m}_{36}$ | $\dot{m}_{32} h_{32} = \dot{m}_{36} h_{36} + \dot{W}_{KT}$ | $W_{KT} = \eta_{KT} . (h_{32} - h_{36})$ | $h_{36} = h_{32} . (h_{32} - h_{36S}) . \eta_{is,KT}$ |
| Mixer | $\dot{m}_{37} = \dot{m}_{35} + \dot{m}_{36}$ | $\dot{m}_{37} h_{37} = \dot{m}_{35} h_{35} + \dot{m}_{36} h_{36}$ | | |
| Throttle valve, TV | $\dot{m}_{34} = \dot{m}_{35}$ | $\dot{m}_{34} h_{34} = \dot{m}_{35} h_{35}$ | $h_{34} = h_{35}$ | |
| Regenerator, REG | $\dot{m}_{33} = \dot{m}_{34}$ $\dot{m}_{30} = \dot{m}_{38}$ | $\dot{m}_{33} h_{33} + \dot{m}_{38} h_{38} = \dot{m}_{34} h_{34} + \dot{m}_{30} h_{30}$ | $\varepsilon_{REG} = \frac{h_{33} - h_{34}}{h_{33} - h_{38}}$ | $\dot{Q}_{REG} = \dot{m}_{38} . (h_{30} - h_{38})$ |
| Pump2 | $\dot{m}_{38} = \dot{m}_{37}$ | $\dot{m}_{37} h_{37} + \dot{W}_{P2} = \dot{m}_{38} h_{38}$ | $\dot{W}_{P2} = \dot{m}_{37} . (h_{38} - h_{37})$ | |
| HEX1 | $\dot{m}_{13} = \dot{m}_{15}$ $\dot{m}_{26} = \dot{m}_{29}$ | $\dot{m}_{13} h_{13} + \dot{m}_{29} h_{29} = \dot{m}_{15} h_{15} + \dot{m}_{26} h_{26}$ | $\dot{Q}_{HEX1} = \dot{m}_{13} . (h_{13} - h_{15})$ | |
| Steam turbine, ST | $\dot{m}_{26} = \dot{m}_{27}$ | $\dot{m}_{26} h_{26} = \dot{m}_{27} h_{27} + \dot{W}_{ST}$ | $W_{ST} = \eta_{ST} . (h_{26} - h_{27})$ | $h_{27} = h_{26} . (h_{26} - h_{27S}) . \eta_{is,ST}$ |
| Condenser | $\dot{m}_{28} = \dot{m}_{27}$ | $\dot{m}_{28} h_{28} = \dot{m}_{27} h_{27}$ | | |
| Pump1 | $\dot{m}_{28} = \dot{m}_{29}$ | $\dot{m}_{28} h_{28} + \dot{W}_{P1} = \dot{m}_{29} h_{29}$ | $\dot{W}_{P1} = \dot{m}_{28} . (h_{29} - h_{28})$ | |

#### 3.2.3. Exhaust Gas Recirculating system, EGR

The Exhaust Gas Recirculating system (EGR), comprised of N2 and O2, is proposed to progress the efficiency of both the ammonia and the methane Brayton cycles. This innovative system receives the air components and then divides them with a specific rate into the inlet of both air compressors while the fresh dry air is supplied to the cycle. The EGR also supplies the gas components in the reference temperature and pressure. The EGR ratio in the ammonia Brayton cycle is calculated by the fraction of the molar recirculated gas to fresh, dry air supplied into the cycle, as follows [12]:

$$EGR = \frac{\dot{n}_{EGR}}{\dot{n}_{AIR} + \dot{n}_{EGR}} \quad (20)$$

## 4. Results and Discussion

### 4.1. Model validation and results

In this section, to determine the accuracy of the present study, a detailed analysis is conducted amid the current research and the benchmark literature.The focus is on evaluating and discussing the outcomes derived from integrated cycles: the ammonia Brayton cycle,

USC Rankine cycle. Initially, the comparative thermodynamic and environmental analyses are conducted between the components of the proposed Brayton cycle and those of Keller et al. [12].

Similarly, the input and output parameters for the Kalina cycle, which is incorporated into the topping cycle through HEX2, are meticulously calculated and then compared with the data provided by Ghaebi et al. [37]. Furthermore, the analysis extends to the HTSE, as well as the ASR processes, all of which constitute significant subsystems of the proposed integrated system. The results are meticulously compared to the relevant literature: [12], [37] and [23].

According to Tables 6–8, the results of presents work displayed a close consistency with those stated in the mentioned literature, and the results confirmed the validity of the current study. Also, the overall utility calculation results obtained in the current study for the proposed system are listed in Table 9, which is derived from the thermodynamic properties of the states in the overall integrated system shown in Table 10.

**Table 6.** Validating the thermodynamic analysis data obtained in the current study compared to Brayton and USC Rankine cycles presented by Keller et al. [12].

| Parameter | Current study | Literature |
|---|---|---|
| GT net power generation, (kW) | 1434 | 969.4 |
| ST power generation, (kW) | 7769 | 7647 |
| Isentropic efficiency of Air compressor, $\eta_{com}$ (%) | 85 | 85 |
| GT Thermal efficiency (%) | 28.74 | 23.73 |
| ST Thermal efficiency (%) | 45.83 | 46.7 |
| Fuel mass flow rate, $m_f$ (kg/s) | 0.198 | 0.198 |
| Isentropic efficiency of gas turbine, $\eta_{gt}$ (%) | 0.8 | 0.8 |
| Pressure Ratio, PR | 20 | 20 |

**Table 7.** Validating the thermodynamic analysis data obtained in the current study compared to Kalina cycle presented by Ghaebi et al. [37].

| Parameter | Current study | Literature |
|---|---|---|
| Basic ammonia mass fraction, $X_b$ (%) | 90.83 | 90 |
| KC Turbine isentropic efficiency, $\eta_{is,tur}$ (%) | 85 | 85 |
| Turbine expansion ratio, TER | 2.003 | 2 |
| Thermal efficiency (%) | 6.083 | 6.683 |
| KC Turbine Power (kW) | 2302 | 931.83 |
| Working fluid mass flow rate (kg/s) | 14.37 | 14.37 |

**Table 8.** Validating the thermodynamic analysis data obtained in the current study compared to HTSE and ASR, processes presented by Yilmaz et al. [23].

| Parameter | Current study | Literature |
|---|---|---|
| Hydrogen production rate, (kg/s) | 1.219 | 0.04214 |
| Ammonia production rate, (kg/s) | 0.6802 | 0.1596 |
| ASR mass ratio | 4.52 | 4.52 |

**Table 9.** Utility calculation results of the overall proposed system.

| Parameter | Value |
|---|---|
| Net power generation, (kW) | 2165 |
| Overall Thermal efficiency, (%) | 47.83 |
| Process Water rate, (kg/s) | 0.2361 |
| Hydrogen storage rate, (kg/s) | 1.097 |
| Ammonia storage rate, (kg/s) | 1.938 |
| Nitrogen storage rate, (kg/s) | 0.538 |
| Oxygen storage rate, (kg/s) | 0.9166 |
| CC heat load, (kW) | 3316 |
| HRSG heat load, (kW) | 1210 |

**Table 10.** Thermodynamic properties of the states of the proposed integrated system.

| State | $\dot{m}$ [kg/s] | P [bar] | T [K] | h [kJ/kg] | s [kJ/kg.K] |
|---|---|---|---|---|---|
| 1 | 1 | 1 | 298.2 | 301.7 | 6.855 |
| 2 | 1 | 20 | 756.6 | 782.5 | 6.955 |
| 3 | 1.198 | 20 | 2004 | 237.4 | 9.234 |
| 4 | 1.198 | 1 | 1024 | -959.2 | 9.233 |
| 5 | 1.348 | 1 | 400 | -2229 | 7.826 |
| 6 | 1.348 | 1 | 298.2 | -2350 | 7.477 |
| 7 | 0.2361 | 1 | 298.2 | -411.6 | 1.309 |
| 8 | 0.7639 | 1 | 298.2 | -1939 | 6.168 |
| 9 | 0.2259 | 1 | 298.2 | -1939 | 6.168 |
| 10 | 0.538 | 1 | 298.2 | -1939 | 6.168 |
| 11 | 2.136 | 1 | 598.3 | 3125 | 8.304 |
| 12 | 2.136 | 1 | 900 | 3765 | 9.167 |
| 13 | 1.219 | 1 | 900 | 12703 | 69.49 |
| 14 | 0.9166 | 1 | 900 | 600.1 | 1.09 |
| 15 | 1.219 | 1 | 298.2 | 3932 | 53.43 |
| 16 | 1.097 | 1 | 298.2 | 3932 | 53.43 |
| 17 | 0.1219 | 1 | 298.2 | 3932 | 53.43 |
| 18 | 0.5583 | 1 | 298.2 | 309.3 | 6.839 |
| 19 | 0.1219 | 150 | 596.3 | 8368 | 42.79 |
| 20 | 0.5583 | 150 | 596.3 | 624.4 | 6.063 |
| 21 | 0.6802 | 20 | 700 | 2539 | 7.218 |
| 22 | 0.6802 | 20 | 412 | -1488 | 5.782 |
| 23 | 2.136 | 1 | 298.2 | 104.9 | 0.3672 |
| 24 | 0.4821 | 1 | 298.2 | 104.9 | 0.3672 |
| 25 | 0.1981 | 1 | 298.2 | 104.9 | 0.3672 |
| 26 | 5 | 250 | 873 | 3493 | 6.363 |
| 27 | 5 | 0.05 | 306 | 1939 | 6.363 |
| 28 | 5 | 0.05 | 306 | 137.7 | 0.4762 |
| 29 | 5 | 250 | 307.7 | 167.2 | 0.4762 |
| 30 | 14.37 | 35.7 | 307.3 | -2391 | 0.533 |
| 31 | 14.37 | 35.7 | 337.2 | 243.2 | 0.9924 |
| 32 | 10.47 | 35.7 | 337.2 | 311.9 | 1.028 |
| 33 | 3.897 | 35.7 | 337.2 | 314 | 1.024 |
| 34 | 3.897 | 35.7 | 296.6 | 111 | 0.3835 |
| 35 | 3.897 | 17.82 | 296.8 | 111.3 | 0.3943 |
| 36 | 10.47 | 17.82 | 295.5 | 103 | 0.3771 |
| 37 | 14.37 | 35.7 | 296.1 | 106.7 | 0.3797 |
| 38 | 14.37 | 35.7 | 294.4 | 98.71 | 0.3525 |

### 4.2. Parametric study results

This section studies the main thermodynamic properties, including air-to-fuel ratio (ATF), equivalence ratio (φ), fuel mass flow rate, inlet air temperature within the Brayton cycle, turbine expansion ratio (TER) of the Kalina cycle, and compressor pressure ratio (PR), etc. Subsequently, the influence of variations on various thermodynamic parameters of the proposed integrated system is investigated. These parameters include thermal efficiency and net output power of the overall system and the subsystems.

#### 4.2.1. The impact of equivalence ratio on TIT temperature at various EGR values

In this section, The impact of equivalence ratio on TIT temperature at various EGR values was investigated. As depicted in Fig. 2, a

discernible upward trend in gas turbine inlet temperature (TIT) becomes evident as the equivalence ratio (φ) increases across all three EGR ratios. Notably, when EGR is set at 0.2, the lowest temperature is observed at the exit of the combustion chamber. Introducing additional nitrogen into the air-fuel mixture results in an elevation of the combustion product temperatures. Consequently, for EGR values exceeding 0.2, the temperature of the products surpasses 4000K, giving rise to challenges related to cost and material constraints in both the combustion chamber and the gas turbine.

The pink vertical line in the graph signifies the optimum equivalence ratio, occurring at φ=1.2. Under ideal circumstances, the optimal EGR value is determined to be 0.29. This analysis sheds light on the intricate relationship between equivalence ratio, EGR, and gas turbine inlet temperature, emphasizing the significance of achieving a balance to mitigate operational challenges and enhance overall system efficiency.

4.2.2. The impact of equivalence ratio on power generation at various EGR values

As depicted in Fig. 3, the impact of equivalence ratio on the output power of gas turbine and overall integrated system was investigated at various EGR values. As can be seen, an increase in the equivalence ratio demonstrates a consistent trend of diminishing power production for both the gas turbine and the overall system across all three EGR ratios. Remarkably, when EGR is set at 0.2, the most significant reduction in power output is observed for both the individual gas turbine and the entire system. Conversely, at the highest nitrogen recirculation rate into Brayton cycle with EGR set at 0.6, the least decrease in power production is evident for both the gas turbine and the overall system.

The graphical representation indicates that at EGR=0.2, particularly in the rich region of ammonia fuel mixture, a substantial decrease in power production is observed due to reduced air volume and incomplete combustion. In practical terms, the gas turbine system experiences a notable decline, rendering it incapable of power production and achieving optimal thermal efficiency.

Under optimal conditions characterized by an equivalence ratio of φ=1.2 and EGR=0.29, the net power production of the gas turbine is measured at 1.43 MW, accompanied by a gas turbine efficiency of $\eta_{th.BC}$=28.7%. These results signify the effectiveness of the specified conditions in maximizing power output and efficiency within the gas turbine system.

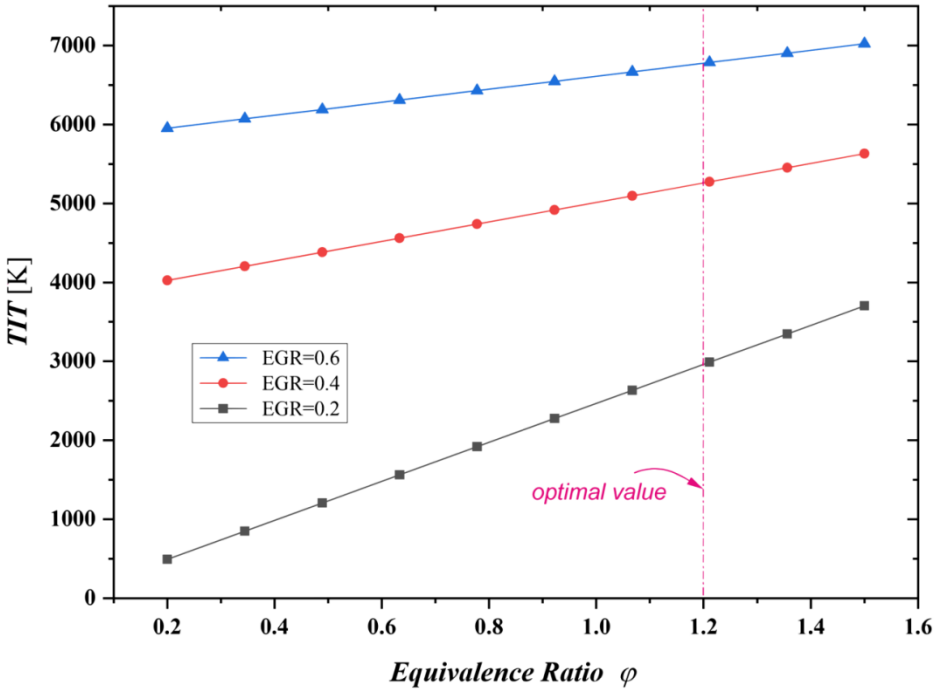


**Fig. 2.** The impact of equivalence ratio on TIT temperature at various EGR values.

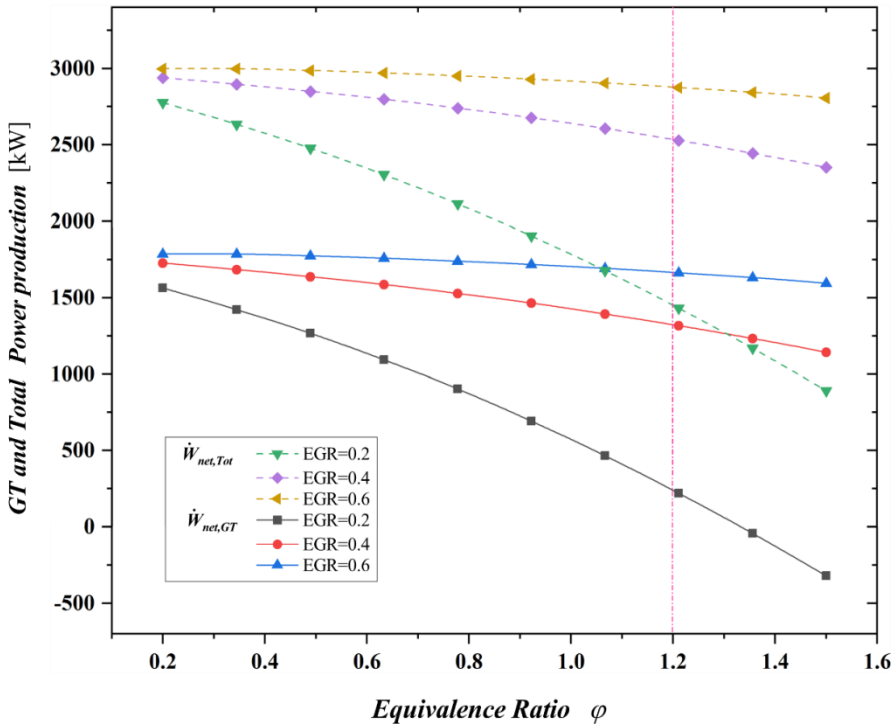


**Fig. 3.** The impact of equivalence ratio on power generation at various EGR values.

4.2.3. The impact of equivalence ratio on the thermal efficiencies at various EGR values.

Fig. 4 displays the impact of equivalence ratio on the thermal efficiencies of gas turbine and overall integrated system was investigated at various EGR values. In accordance with the figure, an elevation in the equivalence ratio is observed to correlate with a reduction in both the thermal efficiency of the gas turbine and the overall system, across all EGR ratios. It is notable that within the rich region (φ<1), the thermal efficiency values on all curves exhibit irrational behavior. Upon transitioning into the sparse region (φ>1), the thermal efficiencies for both the gas turbine and the entire system assume more realistic values. In the rich region, at EGR=0.2, the gas turbine and the entire system exhibit their lowest thermal efficiency, while the peak thermal efficiency in this region is associated with EGR=0.6.

The shorter curves on the graph represent valid yield values for the respective curve, with the excluded points deemed impractical. Generally, an escalation in the equivalence ratio corresponds to a decrease in the quantity of air within the fuel mixture, leading to a diminishing combustion quality over time. Consequently, the decline in efficiency is attributed to suboptimal combustion conditions.

At the optimal point of the equivalence ratio, i.e., φ = 1.2, and with EGR set at 0.29, complete combustion is achieved within the combustion chamber, resulting in an overall system efficiency of $\eta_{th.sys}$ = 47.8%.

4.2.4. The impact of equivalence ratio on the performance of Kanlina and Rankine cycles.

In this section, The impact of equivalence ratio on the performance of Kanlina and Rankine cycles was investigated. As shown in Fig. 5, an increase in the equivalence ratio within the Brayton cycle corresponds to a rise in the temperature of combustion products. This elevation subsequently induces an increase in the specific entropy of fluids utilizing waste heat through HEX1 and HEX2 in the ammonia Brayton cycle. Consequently, a general trend emerges where an augmented equivalence ratio contributes to heightened power rates within the Kalina and Rankine cycles, thereby resulting in an improvement in the thermal efficiency of these two cycles.

Examining the figure, optimal conditions for the Brayton ammonia cycle, characterized by an optimal nitrogen gas ratio (EGR=0.296), reveal that the lowest levels of power production and thermal efficiency for the Kalina and Rankine cycles occur at a specific equivalence ratio of 0.2. Conversely, the highest values are attained at the terminal point of φ=1.6. At the optimal equivalence ratio of φ=1.2, the net power generation in the Rankine and Kalina cycles equals 7769 kW and 2302 kW, respectively. Additionally, the thermal efficiency in the Rankine and Kalina cycles at this optimal point stands at 45.83% and 6.08%, respectively.

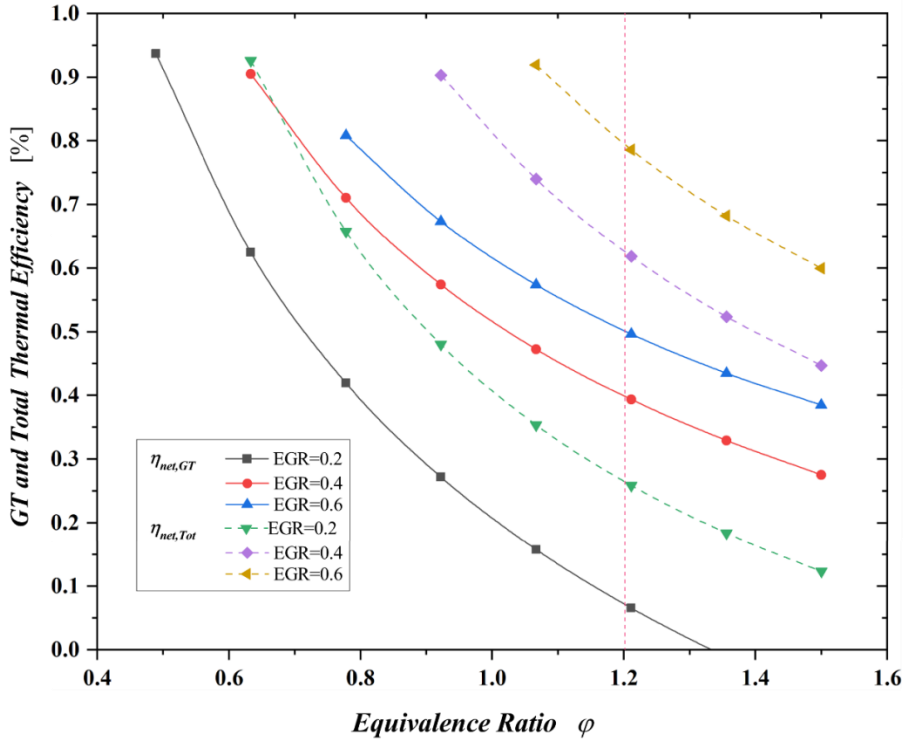


**Fig. 4.** The impact of equivalence ratio on thermal efficiency at various EGR values.

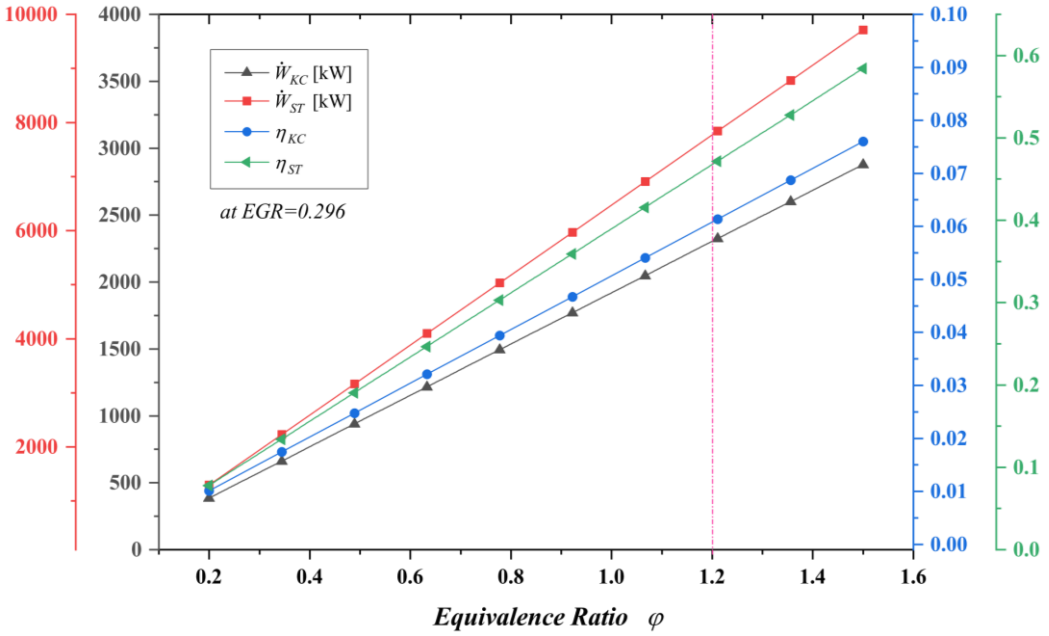


**Fig. 5.** The impact of equivalence ratio on the performance of Kanlina and Rankine cycles.

#### 4.2.5. The impact of water supply ($m_{31}$) on ASR and HTSE flows production

In this section, we explored the influence of varying the water flow rate supplied to High-Temperature Steam Electrolysis (HTSE) on the generation of different gases in the Autothermal Steam Reforming (ASR) and HTSE processes, as illustrated in Fig. 6. As indicated by the figure, there is a discernible correlation between an increase in the mass flow rate of water entering the preheater (designated as) and a consistent upward trend across all depicted curves. The minimum values for the production of oxygen, hydrogen, ammonia, and the necessary nitrogen for the ASR reaction occur at $m_{23} = 1\,kg/s$. Subsequently, with an increment in the water flow rate to $m_{23} = 2\ kg/s$, there is a corresponding growth in the mass flows mentioned above.

This observed trend amplification can be attributed to the direct dependence of the electrolysis process and ammonia synthesis on the availability of water. With an increased influx of water into the HTSE system, there is a corresponding intensification in the production of oxygen and hydrogen. Additionally, an augmented quantity of hydrogen entering the ammonia reactor is inherently linked to the availability of nitrogen as a reactant. Consequently, the rate of ammonia synthesis also experiences an increase. In the proposed ASR and HTSE system, at $m_{23} = 1.143\,kg/s$, the rates of oxygen and hydrogen production are $m_{14} = 0.4906\,kg/s$ and $m_{16} = 0.5872\,kg/s$, respectively. Simultaneously, the quantity of nitrogen necessary for the ASR reaction and the ultimate production of ammonia equals $m_{18} = 0.2988\,kg/s$ and $m_{21} = 0.3641\,kg/s$, respectively.

#### 4.2.6. The impact of basic ammonia concentration of Kalina cycle.

In this section, we conducted a comprehensive analysis of the impact of variations in the basic ammonia concentration on the thermodynamic characteristics of both the Kalina cycle and the proposed multigeneration system, as depicted in Fig. 7. The presented data reveal a crucial observation: an increase in the basic ammonia concentration, denoted as$X_b$, within the range of $80 < X_b < 91$, results in a noticeable decreasing trend across all the graphs. In stark contrast, the figure illustrates a state of relative constancy in the domain of $X_b > 91$. This distinctive pattern strongly indicates the existence of an optimal value of basic ammonia concentration within $X_b > 91$, a point at which the power generation potential of the Kalina cycle and the multigeneration system converges at approximately 0.6 MW and 9.5 MW, respectively. Simultaneously, both the efficiencies of the Kalina cycle and the multigeneration system demonstrate noteworthy performance, with values of 7% and 58%, respectively.

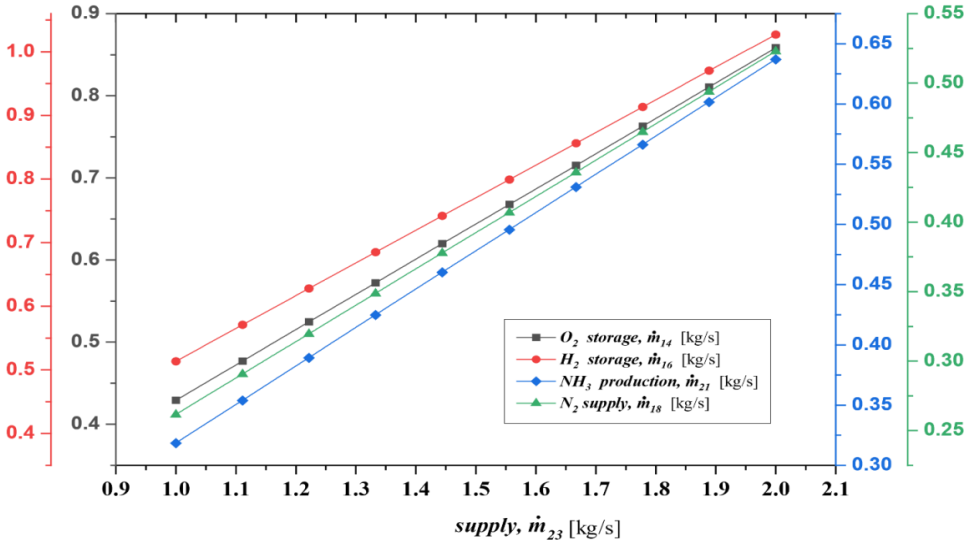


**Fig. 6.** The impact of water supply on ASR and HTSE flows production.

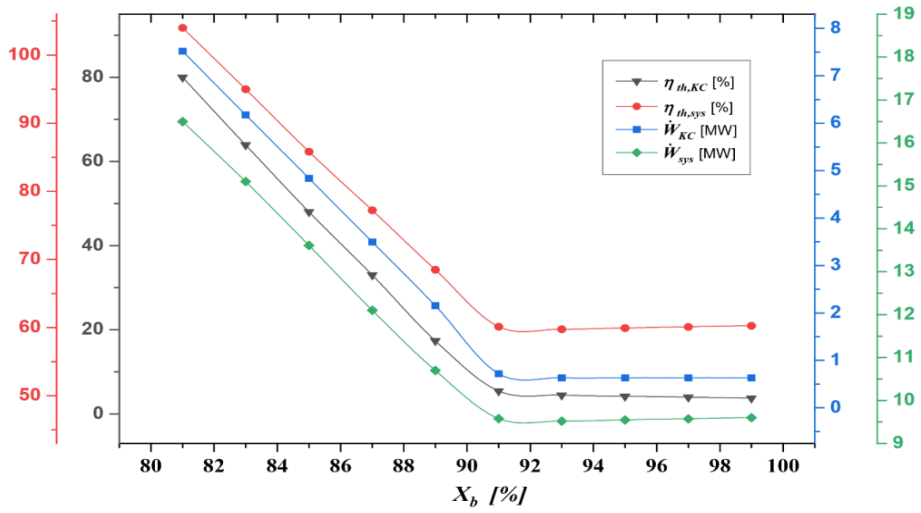


**Fig. 7.** The impact of basic ammonia concentration of Kalina cycle, ($X_b$).

In summary, a careful examination of Fig. 7 underscores the positive impact of a higher ammonia concentration ($X_b > 91$) within the water-ammonia solution on increasing both power output and the thermal efficiency of the integrated system. This finding constitutes a significant contribution to understanding the optimal conditions for ammonia concentration in the proposed energy system.

4.2.7. The impact of turbine expansion ration (TER) of Kalina cycle.

The investigation delved into the impact of variations in Turbine Expansion Ratio (TER) on both the Kalina cycle performance and the overall proposed system, as demonstrated in Fig. 8. A discernible trend emerges from the figure: within the range of 1.8 < TER < 2.1, there is a consistent and noticeable decrease observed across all graphical representations. In contrast, for TER values surpassing 2.1, a uniform trend is observed across all curves. Within these conditions, an optimal Turbine Expansion Ratio emerges at TER > 2.1, where both the power generation of the Kalina cycle and the overall system converge at approximately 0.4 MW and 9.4 MW, respectively. Additionally, during this interval, the efficiencies of the Kalina cycle and the overall system reach 6.5% and 58%, respectively.

In summary, the diagram distinctly illustrates that an augmentation in TER leads to an increased pressure difference within the Kalina turbine. However, it is noteworthy that this elevation does not translate into improvements in power production or the efficiency of the proposed integrated system.

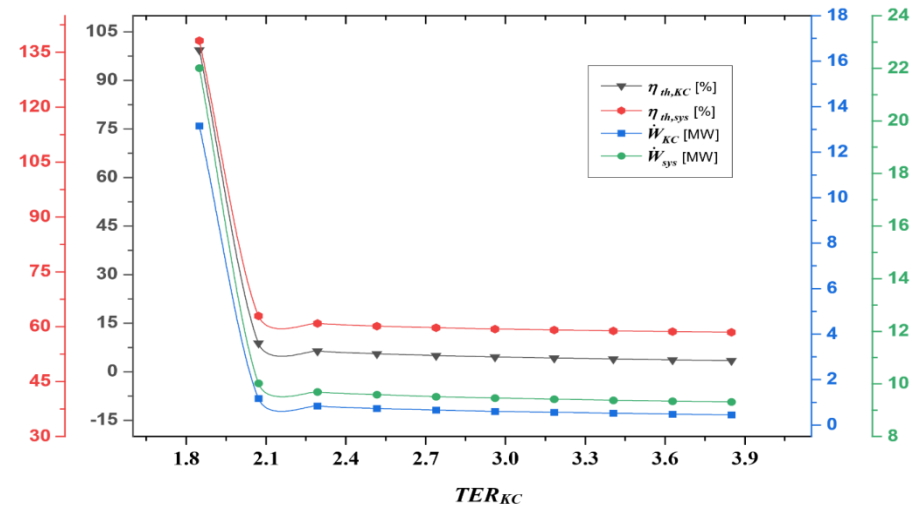


**Fig. 8.** The impact of turbine expansion ratio (TER) of Kalina cycle.

## 5. Conclusion

In this investigation, we examined the development of a self-sustained Combined Heat and Power (CHP) energy system, exploring an innovative integrated approach. The system harnessed ammonia as a fuel within a Brayton cycle, interconnecting various subsystems, including the Kalina and Rankine cycles, High-Temperature Steam Electrolysis (HTSE), and an ammonia synthesis reactor. Our primary objective was to minimize external dependencies by locally sourcing water and fuel, thereby reducing the environmental impact and fortifying energy sustainability.

Therefore, the adaptability of the proposed system to various parameters such as equivalence ratio, air-to-fuel ratio (ATF), and more was practiced. These parameters exhibited a significant impact on thermodynamic attributes, including thermal efficiency, net power output, and combustion products. Our investigation revealed several key insights, including the intricate interplay of these parameters, trade-offs between EGR, equivalency ratio, efficiency, and the critical need to maintain an optimal equilibrium among various design parameters. After a comprehensive performance assessment, we draw the following multifaceted conclusions:

- The thermal efficiency of the Brayton cycle, Kalina cycle, and USC Rankine cycle was found to be 28.7%, 6.08%, and 45.8%, respectively, while the integrated system demonstrated an exceeded efficiency of 47.8%.
- Despite the net power generation output of the proposed CHP system being 2.165 MW, other subsystems, including the Brayton cycle, Kalina cycle, and USC Rankine cycle, recorded values of 1.4 MW, 7.77 MW, and 2.3 MW, respectively.
- Power demand for HTSE emerged as the major consumer of generated power in the proposed system, surpassing 7 MW.
- Increasing the Turbine Inlet Temperature (TIT) enhanced the efficiency and net power output of the Brayton cycle and the proposed integrated CHP system, attributed to heightened heat input and overall thermal efficiency.
- Elevating the HTSE Inlet Temperature increased the power demand for electrolysis, augmenting the heat load in HEX1 and subsequent power production in the USC steam Rankine cycle.
- A higher ammonia concentration in the Kalina cycle positively impacted power generation capacity and overall efficiency.

To summarize, this study uncovered the potential of an ammonia Brayton cycle as a carbon-free energy system. It is noteworthy that developing the proposed CHP system, considering exergy and economic aspects, will be explored in future studies.

## References

[1] "Global Energy & CO2 Status Report 2019," 2019. [Online]. Available: https://www.iea.org/reports/global-energy-co2-status-report-2019. [Accessed 2023 10 28].

[2] C. Wiesen, "Special Report on Global Warming of 1.5°C," The Intergovernmental Panel on Climate Change. IPCC, The United Nations, 2017.

[3] Lund H., Mathiesen B.V., "Energy system analysis of 100% renewable energy systems—The case of Denmark in years 2030 and 2050," Energy, vol. 34, no. 5, pp. 524-531, 2009.

[4] Yilmaz F., Ozturk M., Selbas R., "Development and performance examination of an integrated plant with desalination process for multigeneration purposes," Energy Conversion and Management, vol. 240, p. 114275, 2021.

[5] Tabrizi Z.H., Mohammadourfard M., Akkurt G.G., Heris S.Z., "Energy, exergy, exergoeconomic, and exergoenvironmental (4E) analysis of a new bio-waste driven multigeneration system for power, heating, hydrogen, and freshwater production: Modeling and a case study in Izmir," Energy Conversion and Management, vol. 288, p. 117130, 2023.

[6] Ghasemiasl R., Abhari M.K., Javadi M.M., Gomashi H., "4E investigating of a combined power plant and converting it to a multigeneration system to reduce

environmental pollutant production and sustainable development," Energy Conversion and Management, vol. 245, p. 114468, 2021.

[7] D'Amore F., Nava F., Colbertaldo P., Visconti C.G., Romano M.C., "Turning CO2 from fuel combustion into e-Fuel? Consider alternative pathways," Energy Conversion and Management, vol. 289, p. 117170, 2023.

[8] Valera-Medina A., Morris S., Runyon J., Pugh D.G., Marsh R., Beasley P., Hughes T., "Ammonia, Methane and Hydrogen for Gas Turbines," Energy Procedia, vol. 75, pp. 118-123, 2015.

[9] Ávila C.D., Cardona S., Abdullah M., Younes M., Jamal A., Guiberti T.F., Roberts W.L., "Experimental assessment of the performance of a commercial micro gas turbine fueled by ammonia-methane blends," Applications in Energy and Combustion Science, vol. 13, p. 100104, 2023.

[10] Xiao, H., Wang, Z., Valera-Medina, A. et al., "Study on Characteristics of Co-firing Ammonia/Methane Fuels under Oxygen Enriched Combustion Conditions," J. Therm. Sci., vol. 27, p. 270–276, 2018.

[11] Valera-Medina A., Marsh R., Runyon J., Pugh D., Beasley P., Hughes T. , BowenT., "Ammonia–methane combustion in tangential swirl burners for gas turbine power generation," Applied Energy, vol. 185, pp. 1362-1371, 2017.

[12] Keller M., Koshi M., Otomo J., Iwasaki H., Mitsumori T., Yamada K., "Thermodynamic evaluation of an ammonia-fueled combined-cycle gas turbine process operated under fuel-rich conditions," Energy, vol. 194, p. 116894, 2020.

[13] Pirmohamadi A., Ziapour B.M. , "Proposal of a novel ammonia brayton cycle integrated with a methane/hydrogen brayton cycle; Thermodynamic and environmental impacts assessments," Energy Equipment and Systems, vol. 11, no. 1, pp. 95-122, 2023.

[14] Okafor E.C., Yamashita H., Hayakawa A., et al., "Flame stability and emissions characteristics of liquid ammonia spray co-fired with methane in a single stage swirl combustor," Fuel, vol. 287, p. 119433, 2021.

[15] Guteša Božo M. , Vigueras-Zuniga M.O., Buffi M., Seljak T., Valera-Medina A., "Fuel rich ammonia-hydrogen injection for humidified gas turbines," Applied Energy, vol. 251, p. 113334, 2019.

[16] Guteša Božo M. , Mashruk S., Zitouni S., Valera-Medina A., "Humidified ammonia/hydrogen RQL combustion in a trigeneration gas turbine cycle," Energy Conversion and Management, vol. 227, p. 113625, 2021.

[17] Da Rocha R.C., Costa M., Bai X.S.,, "Chemical kinetic modelling of ammonia/hydrogen/air ignition, premixed flame propagation and NO emission," Fuel, vol. 246, pp. 24-33, 2019.

[18] Honzawa T., Kai R., Okada A., Valera-Medina A., Bowen P.J., KuroseR., "Predictions of NO and CO emissions in ammonia/methane/air combustion by LES using a non-adiabatic flamelet generated manifold," Energy, vol. 186, p. 115771, 2019,.

[19] Valera-Medina A., Gutesa M., Xiao H., Pugh D., Giles A., Goktepe B., Marsh R., Bowen P., "Premixed ammonia/hydrogen swirl combustion under rich fuel conditions for gas turbines operation," International Journal of Hydrogen Energy, vol. 44, no. 16, pp. 8615-8626, 2019.

[20] Xiao H.,Valera-Medina A., "Chemical Kinetic Mechanism Study on Premixed Combustion of Ammonia/Hydrogen Fuels for Gas Turbine Use," ASME. J. Eng. Gas Turbines Power, vol. 139, no. 8, p. 081504, 2017.

[21] Su B., Huang Y., Wang Y., Huang Z., Yuan S., Huang Q., Xu Z., Lin F., "Novel ammonia-driven chemically recuperated gas turbine cycle based on dual fuel mode," Applied Energy, vol. 343, p. 121184, 2023.

[22] Wang Y., Liu J., Wang L., Fu Z., Weng P., "Non-premixed combustion and NOX emission characteristics in a micro gas turbine swirl combustor fueled by methane and ammonia at various heat loads," Heliyon, vol. 9, no. 3, p. e14521, 2023.

[23] Yilmaz F., Ozturk M., Selbas R., "Thermodynamic performance analysis and environmental impact assessment of an integrated system for hydrogen and

ammonia generation," International Journal of Hydrogen Energy, vol. 46, no. 57, 2021.

[24] Yilmaz F., Ozturk M., Selbas R., "Development and performance examination of an integrated plant with desalination process for multigeneration purposes," Energy Conversion and Management, vol. 240, p. 114275, 2021.

[25] He W., Namar M.M., Li Z., Maleki A., Tlili I., Safdari Shadloo M., "Thermodynamic analysis of a solar-driven high-temperature," Appl Therm Eng, vol. 172, 2020.

[26] AlZahrani A.A., Dincer I., "Exergoeconomic analysis of hydrogen production using a standalone high-temperature electrolyzer," Int J Hydrogen Energy, vol. 46 , no. 27, pp. 13899-13907, 2021.

[27] Anvari S., Mahian O., Taghavifar H., Wongwises S., Desideri U., "4E analysis of a modified multigeneration system designed for power, heating/cooling, and water desalination," Applied Energy, vol. 270, p. 115107, 2020.

[28] Eldeib A., Luqman M., Bicer Y., Al-Ansari T.A.,, "Thermodynamic design and analysis of a multigeneration system to support sustainable dairy farming," Energy Conversion and Management, vol. 18, p. 100363, 2023.

[29] Liu Q., Arabkoohsar A., Liu Y., He Z., "Techno-economic analysis of a liquid air energy storage system combined with calcium carbide production and waste heat recovery," Journal of Energy Storage, vol. 60, p. 106689, 2023.

[30] Pulla B.P., Nutakki T.U.K., Albani A., Agrawal M.K., Begum M.Y., Han W., "Comprehensive technical study of a novel polygeneration arrangement using natural gas power plant and geothermal energy for producing electricity, heat, fresh water, and methanol," Process Safety and Environmental Protection, vol. 180, pp. 98-121, 2023.

[31] Ding G.C.,JI P., GENG M.Y.,, "Technical assessment of Multi-generation energy system driven by integrated renewable energy Sources: Energetic, exergetic and optimization approaches," Fuel, vol. 331, p. 125689, 2023.

[32] Bicer Y., Dincer I., "Development of a new solar and geothermal based combined system for hydrogen production," Sol Energy ;127:, vol. 127, pp. 269-284, 2016.

[33] Acar C., Dincer I., "Investigation of a new integrated system for multiple outputs with hydrogen and methanol," International Journal of Hydrogen Energy, vol. 46, no. 6, pp. 4699-4715, 2021.

[34] Siddiqui O., Ishaq H., Dincer I., "A novel solar and geothermal based trigeneration system for electricity generation,hydrogen production and cooling," Energy Convers Manag, vol. 198, p. 111812, 2019.

[35] Akrami E, Chitsaz A, Nami H, Mahmoudi SMS., "Energetic and exergoeconomic assessment of a multi-generation energy system based on indirect use of geothermal energy," Energy, vol. 124, pp. 625-639, 2017.

[36] Bet Sarkis R., Zare V., "Proposal and analysis of two novel integrated configurations for hybrid solar-biomass power generation systems: thermodynamic and economic evaluation," Energy Convers Manag, vol. 160, pp. 411-425, 2018.

[37] Ghaebi H., Namin A.S., Rostamzadeh H., "Exergoeconomic optimization of a novel cascade Kalina/Kalina cycle using geothermal heat source and LNG cold energy recovery," Journal of Cleaner Production, vol. 189, pp. 279-296, 2018.

[38] Tao J., Dong W., Qiu B., Xu C., Liu Y., Chu H., "Effect of Ammonia on Laminar Combustion Characteristics of Methane−Air Flames at Elevated Pressures," ASC OMEGA, vol. 7, p. 15326−15337, 2022.

[39] Pirmohamadi A., Ghaebi H., Ziapour B.M. , Ebadollahi M., "Exergoeconomic Analysis of a Novel Hybrid System by Integrating the Kalina and Heat Pump Cycles with a Nitrogen Closed Brayton System," Energy Reports, vol. 7, pp. 546-564, 2021.

[40] Kobayashi H., Hayakawa A., Kunkuma K.D., Somarathne A., Okafor E.C., "Science and technology of ammonia combustion," Proceedings of the Combustion Institute, vol. 37, p. 109–133, 2019.